HHS Public Access

Author manuscript

Brain Struct Funct. Author manuscript; available in PMC 2016 April 29.

Published in final edited form as:

Brain Struct Funct. 2015 March ; 220(2): 1173–1186. doi:10.1007/s00429-014-0710-3.

Development of Human Brain Cortical Network Architecture during Infancy

Wei Gao[1], **Sarael Alcauter**[1], **J Keith Smith**[2], **John Gilmore**[3], and **Weili Lin**[1]

[1]Department of Radiology and Biomedical Research Imaging Center, University of North Carolina at Chapel Hill, N.C., U.S.A

[2]Department of Radiology, University of North Carolina at Chapel Hill, N.C., U.S.A

[3]Department of Psychiatry, University of North Carolina at Chapel Hill, N.C., U.S.A

Abstract

The brain's mature functional network architecture has been extensively studied but the early emergence of the brain's network organization remains largely unknown. In this study, leveraging a large sample (143 subjects) with longitudinal rsfMRI scans (333 datasets), we aimed to characterize the important developmental process of the brain's functional network architecture during the first two years of life. Based on spatial independent component analysis and longitudinal linear mixed effect modeling, our results unveiled the detailed topology and growth trajectories of nine cortical functional networks. Within networks, our findings clearly separated the brains networks into two categories: primary networks were topologically adult-like in neonates while higher-order networks were topologically incomplete and isolated in neonates but demonstrated consistent synchronization during the first two years of life (connectivity increases 0.13~0.35). Between networks, our results demonstrated both network-level connectivity decreases (−0.02~−0.64) and increases (0.05~0.18) but decreasing connections (n=14) dominated increasing ones (n=5). Finally, significant sex differences were observed with boys demonstrating faster network-level connectivity increases among the two frontoparietal networks (growth rate was 1.63e-4 per day for girls and 2.69e-4 per day for boys, p<1e-4). Overall, our study delineated the development of the whole brain functional architecture during the first two years of life featuring significant changes of both within- and between-network interactions.

INTRODUCTION

The mature human brain features not only specialized but also interacting functional networks (Friston et al. 1993). Such network organization facilitates both single-modal processing and multi-modal integration. Disruptions of the brain's network structure are associated with neurodevelopmental (Dickstein et al. 2010; Di Martino et al. 2010; Fair et al. 2010) and neurodegenerative brain disorders (Andrews-Hanna et al. 2007; Greicius et al. 2004; Rombouts et al. 2005; Wang et al. 2012). Thus, a better understanding of the brain's

Corresponding Author: Wei Gao, Ph.D., University of North Carolina at Chapel Hill, Department of Radiology and Biomedical Research Imaging Center, Rm 3105, Bioinformatics Building, Chapel Hill, NC 27599, TEL: 919-843-7672, FAX: 919-843-4456, wgao@email.unc.edu.

network organization is of critical importance. The resting-state functional magnetic resonance imaging (rsfMRI) (Biswal et al. 1995) has been proven to be a powerful tool in delineating the complex architecture of the brain's functional neural networks. Based on a data-driven probabilistic independent component analysis (ICA) approach, Damoiseaux and colleagues (Damoiseaux et al. 2006) identified a set of resting state networks (RSNs) that are consistently observed across healthy normal subjects. Using a clustering approach, Yeo et al (Yeo et al. 2011) similarly defined a functional network parcellation of the entire cerebral cortex that shows largely consistent spatial topologies as those defined by Damoiseaux et al. Importantly, Smith et al (Smith et al. 2009) reported ten functional networks showing highly consistent topologies between resting and activation states, suggesting a converging brain network architecture between resting and task dynamics. These studies provide parsimonious representations of the whole brain functional system that have far reaching benefits to our understanding of both normal and abnormal brain functional mechanisms.

While the above-mentioned studies have revealed the mature brain functional network architecture, our understanding of the early brain functional developmental process remains largely in the dark and deserves similar delineation (Power et al. 2010; Fair et al. 2008; Fair et al. 2009; Kelly et al. 2009; Supekar et al. 2009; Gao et al. 2011). Recent studies have begun to illuminate this area by delineating the emergence of individual functional networks such as the visual network (Doria et al. 2011; Lin et al. 2008; Fransson et al. 2007), the sensorimotor network (Lin et al. 2008; Doria et al. 2011), the default-mode network (Raichle et al. 2001; Gao et al. 2009; Fair et al. 2008; Doria et al. 2011), and the dorsal attention network (Corbetta and Shulman 2002; Gao et al. 2012). These studies suggest earlier maturation of primary functional networks, which are already synchronized at birth (Smyser et al. 2010; Fransson et al. 2007), than higher-order ones, which experience prolonged postnatal synchronization processes (Gao et al. 2009; Gao et al. 2012; Fair et al. 2008). Despite these exciting findings, critical questions remain. For example, without a longitudinal design, the network-specific growth trajectories during the critical early development period are difficult to delineate. Moreover, given the increasing awareness of the importance of functional interactions among large-scale functional networks in both normal (Elton and Gao In Press; Gao et al. 2013; Gao and Lin 2012; Spreng et al. 2010; Fornito et al. 2012) and abnormal brain functioning (Sripada et al. 2012; Stern et al. 2012), a systematic examination of all possible functional networks and their corresponding network-level interactions during early developmental period may be especially important for advancing our understanding of the brain's functional mechanisms. Finally, given the apparent behavioral differences between boys and girls (Gaulin 1993; Kail 1993), potential sex effects on the brain's functional network development in early childhood are also interesting scientific questions to explore.

In this study, we aimed to address these questions by examining a large cohort of infants with longitudinal scans of rsfMRI at birth, one-year, and two-years of age (n=143, each infant scanned at least twice, total number of scans=333). With the aim to delineate the development of the whole brain network architecture, probabilistic ICA was adopted to simultaneously delineate all possible functional networks within each age group. Longitudinal linear mixed effect modeling was conducted to characterize the growth

trajectories of both the intra- and internetwork functional connectivity. Finally, sex differences on the development of the brain's functional network connectivity were also explored. For intra-network synchronization, we hypothesized that primary networks would feature adult-like topology at birth while higher-order networks would show largely incomplete structure in neonates but dramatic synchronization during the first two years of life (Gao et al. 2011; Gao et al. 2012; Gao et al. 2009). For internetwork connectivity, both network-level interaction decreases and increases were expected (Tau and Peterson 2010). Finally, given the documented relationship between functional connectivity and sex differences in different behaviors (Gaulin 1993; Kail 1993; Kilpatrick et al. 2006; Tomasi and Volkow 2012), we also hypothesized the emergence of sex differences on the growth of network functional connectivity during early childhood.

MATERIALS AND METHODS

Subjects

Participants were part of a large study characterizing brain development in normal and high-risk children (Gilmore et al. 2012; Alcauter et al. 2013; Gao et al. 2011; Gao et al. 2012; Gao et al. 2009). Informed written consent was obtained from the parents of all participants and all study protocols were approved by the University of North Carolina at Chapel Hill Institutional Review Board. We retrospectively identified 143 healthy normal subjects (77 males) scanned at least twice during the first two years of life: neonates (n=112, mean age= 33 ± 19 days), 1-year olds (n=129, mean age= 13.3 ± 1.2 months) and 2-year olds (n=92, mean age= 25.4 ± 1.1 months). The distribution of ages at which the subjects were longitudinally scanned is shown in Table 1. Inclusion criteria were birth between gestational age of 35 and 42 weeks, appropriate weight for the gestational age and the absence of major pregnancy and delivery complications as defined in the exclusion criteria. Exclusion criteria included maternal pre-eclampsia, placental abruption, neonatal hypoxia, any neonatal illness requiring greater than a one day stay at a neonatal intensive care unit, mother with HIV, mother using illegal drugs/narcotics during pregnancy, and any chromosomal or major congenital abnormality. Before imaging, subjects were fed, swaddled, and fitted with ear protection. All subjects were in a natural sleep state during the imaging session. A board-certified neuroradiologist (JKS) reviewed all images to verify that there were no apparent abnormalities.

Imaging

All images were acquired with a 3T MR scanner (Siemens Medical systems, Erlangen, Gernamy). Resting state functional MRI (rsfMRI) was acquired using a T2*-weighted EPI sequence: TR=2s, TE=32ms, 33 slices, voxel size of 4×4×4 mm^3. 150 volumes were acquired in a 5 minutes scan. In order to provide anatomical reference, structural images were acquired using a 3D MP-RAGE sequence (TR=1820ms, TE=4.38 ms, inversion time=1100ms), with a voxel size of 1×1×1 mm^3.

Data Analysis

Functional data were preprocessed using FMRIBs Software Libraries (FSL, v 4.1.9) (Smith et al. 2004). The preprocessing steps included discarding the first ten volumes, slice timing

correction, motion correction, high pass (> 0.01 Hz) and low pass filtering (< 0.08 Hz). Mean signal from white matter, cerebrospinal fluid, whole brain, and six motion parameters were removed using linear regression. Adaptive spatial smoothing according to different brain sizes was performed with a Gaussian kernel with sigma = 1.7, 3.3 and 3.8 mm for neonates, 1-year, and 2-year olds, respectively. In order to further reduce the effect of motion on functional connectivity measures, the "scrubbing" approach by controlling the global measure of signal change (0.5 %) and framewise displacement (FD, 0.5mm) were carried out as proposed by Power et al. (2012a). A lower limit of more than 90 volumes remaining after this scrubbing process was set as one of the inclusion criteria. Given the recent suggestion of more stringent scrubbing threshold (FD<0.2mm and signal change <0.3%) (Satterthwaite et al. 2012; Satterthwaite et al. 2013; Power et al. 2013), the results from the more stringent threshold were also obtained for comparison. For each subject and session, after an initial rigid alignment between functional data and the T1 high resolution structural image, a nonlinear transformation field was obtained from the individual T1 image to the corresponding age-specific template using FSL (Smith et al. 2004). The template images were obtained from one subject with longitudinal scans at 2 weeks, 1-year and 2-year olds. The combined transformation field was used to warp the preprocessed rsfMRI data to the template. This study focused on the development of cerebral cortical networks so only areas covered by cortical brain regions were extracted for subsequent analysis using UNC infant atlases (Shi et al. 2011), which were registered to the longitudinal template using a nonlinear transformation with FSL (Smith et al. 2004).

To explore the functional network structure of the human brain cortex during infancy, probabilistic ICA was carried out in each of the three age groups separately using FSL. Specifically, following concatenation of time series from individual subjects, group fMRI data was decomposed into 21, 22 and 24 independent components for neonates, 1- and 2-year olds, respectively, using the FSL's melodic algorithm. The number of components was estimated using the Laplace approximation (implemented in FSL's melodic). To better understand the functional relevance of all ICA defined networks and examine when and how adult-like network topology emerges, 9 adult functional neural networks delineated by Smith et al (Smith et al. 2009) were used as references to group the pediatric components. They include the medial occipital network, the occipital pole network, the lateral visual/parietal network, the default-mode network, the sensorimotor network, the auditory/language network, the salience network, and the two lateralized frontoparietal networks. Note the cerebellum network was excluded given the focus of this study on cortical brain networks. Specifically, infant components were matched, based on spatial similarity, to the adult functional network with which it demonstrated the highest spatial correlation (compared with the remaining 8 networks) and for which the spatial correlation passed a threshold of 0.2. This constrained matching procedure ensured the identification of not only the best match but also a decent match (spatial correlation higher than 0.2). After automatic matching, a visual inspection was carried out and topological correspondence between infant and adult networks was confirmed. Before this spatial matching process, components apparently representing motion artifacts and/or large vessels were identified and excluded. The components that failed to find a match to one of the nine adult functional networks based on the criteria described above were also excluded from subsequent analyses.

To define non-overlapping functional regions from each network for subsequent quantitative analyses, a voxel-wise “winner-takes-all” approach (Buckner et al. 2011; Zhang et al. 2008) was carried out and each voxel in the brain was labeled as belonging to the component within which it demonstrated the highest ICA score comparing with all other included components defined for that group (i.e., components with a detected match with adult reference networks). This procedure yields 21, 23, and 33 functionally defined regions for neonates, 1-year-olds, and 2-year-olds brain, respectively. To establish a common set of ROIs for subsequent quantitative delineation of the network growth trajectories, a second level of “winner-takes-all” parcellation was done to group the regions defined for 2-year-olds into the nine reference adult networks. Specifically, each defined region was labeled as belonging to the network within which the region showed the highest mean ICA score. By doing this we developed a network-level parcellation of the 2-year-old brain which was subsequently used as a template (warped to neonates and 1-year-olds (Shen and Davatzikos 2004)) to quantitatively characterize the development of within- and between-network connectivity. Specifically, mean inter-regional functional connectivity was calculated for each network and each subject to represent within-network synchronization level and longitudinal modeling was conducted to characterize whether and how individual networks become synchronized during the first two years of life. Mean inter-regional connectivity between pairs of regions from two networks was calculated to represent between-network interactions and similarly analyzed.

For longitudinal modeling to delineate the network growth curves, linear mixed-effect (LME) model was selected and implemented in R. Specifically, for each within- and between-network interaction, both a linear model and a log-linear model with age or log(age) as fixed effects plus the intercept and sex terms were built. The log-linear model was tested based on previous findings of more dramatic functional development during the first year than the second for different functional networks (Alcauter et al. 2013; Gao et al. 2012; Gao et al. 2009). Moreover, an interaction term between sex and either age or log(age) was also added to detect potential sex effects on the growth rates. Random effects were added for both the intercept and the age term (either age or log(age)). When the sex by age (or log(age)) interaction term was not significant, reduced models with only the intercept and age term (either age or log(age)) were built to model the main growth effects. For all models, the residual framewise displacement (FD) measure after the previously described scrubbing process was modeled as a covariate of no interest to control for the residual motion artifacts. Akaike information criterion (AIC) was used to gauge whether the linear (i.e age) or log-linear model (i.e., log(age)) with age was a better fit for each measure and the better model was subsequently reported in our results section. Significant effects were defined as $p<0.05$ after FDR correction of all network-level models.

In addition to longitudinal modeling, the cross-sectional representation of the functional connectivity pattern among the 33 defined regions were visualized using spring-embedding plots (Ebbels et al. 2006) based on the age-specific correlation matrices. Specifically, all regional connections were statistically tested (t-test) and only those significantly positive ones ($p<0.05$ after FDR correction in each age group) were modeled and visualized. Spring-embedding plots optimize the spatial location of all nodes in a graph based on their

functional connectivity strengths so that the stronger the functional interaction the closer their spatial locations and *vice versa*.

RESULTS

Sixteen, seventeen, and eighteen components from the neonates, 1yr, and 2yr group, respectively, were successfully grouped into nine adult network categories and were shown in Fig. 1. Consistent with our hypothesis, both the medial visual and sensorimotor network in neonates showed adult-like topology featuring local connectivity within the occipital lobe (Fig. 1a) and bilateral connectivity between sensorimotor cortices (Fig. 1e), respectively. All other neonatal components demonstrated local or bilateral homologous connections but were far from adult-like at this early age primarily because of the spatially distributed nature of these higher-order networks in their mature form (Fig. 1). Note the occipital pole network observed in adults (also in the two later age groups) did not have a match in neonates. The matching of multiple components with the same adult network seemed to represent different subparts of the same network although one should be cautious that this does not imply the existence of the complete network in infants. In one-year-olds, except for the sensorimotor network, there were dramatic changes for all other networks. For instance, the medial visual network and the occipital pole network were clearly separated. Adult-like network topology arose for all other networks with at least one component within each category (Fig. 1) demonstrating higher than 0.4 spatial correlation with the corresponding adult network (the highest $r=0.80, 0.73, 0.65, 0.40, 0.43, 0.48, 0.42, 0.64, 0.49$, for each of the nine networks, respectively, $p<1e\text{-}6$ for all pair-wise correlations, Fig. 1) which was consistent with the general emergence of adult-like distributed network structures observed at this age. The network structure of 2-year-olds remained highly consistent with that of 1-year-olds with only minor refinements (the highest $r=0.75, 0.71, 0.66, 0.55, 0.41, 0.53, 0.49, 0.62, 0.41$, respectively, $p<1e\text{-}6$ for all pair-wise correlations, Fig. 1). The components that were functionally meaningful but did not match with any of the 9 adult networks were shown in Fig. S1 and those components clearly demonstrating artifacts were presented in Fig. S2.

The functional regions defined using a winner-takes-all approach based on the ICA components defined in each individual group were shown in Fig. 2. Further, the 33 functionally defined regions in 2-year olds were grouped according to the 9 adult reference networks and shown in Fig. 3. Using the 33 regions defined in 2-year olds group as template, the spring-embedding plot of the functional relationship among these regions demonstrated a scattered-to-clustered pattern (Fig. 4a): in neonates, regions within different networks (represented by different colors) were inter-mixed and there was no network clustering pattern except for the sensorimotor network (yellow color); in 1-year-olds, however, nodes with the same color became more grouped while in 2-year-olds, all same-colored nodes formed closely interacting clusters. This qualitative network synchronization pattern was also supported by the quantitative delineation of the growth curves of within-network functional connectivity as shown in Fig. 4b: all within-network connectivity measures, except for that of the sensorimotor network, demonstrated significant log-linear growth during the first two years of life indicating dramatic within-network synchronization. Note the medial visual and occipital pole network were not included in this plot since only one region was observed for each network so there was no intranetwork connectivity measured.

The yearly growth of each network, calculated as the difference of the mean connectivity strength between two consecutive years were presented in Fig. 4c. Again, the non-linear growth trend of was clear: much more dramatic within-network connectivity changes were observed during the first year (connectivity increases ranging from 0.17 to 0.38) than the second (connectivity increases/decreases ranging from −0.06 to 0.05, overall connectivity increases throughout the first two years of life ranging from 0.13 to 0.35). Across the six synchronizing networks, the auditory/language is the fastest growing network followed by lateral visual/parietal, default, right frontoparietal, salience, and left frontoparietal network (Fig. 4c).

For between-network interactions (Fig. 5), 14 out of 36 were found to be significantly decreasing while only 5 were increasing (Fig. 5a). Specifically, the 14 inter-network connectivity decreases were found among primary networks (n=3), between primary and association networks (n=7), and among higher-order cognitive networks (n=4). In contrast, the 5 network-level integrations existed only among association networks (i.e., Frontoparietal R-default, Frontoparietal R-Frontoparietal L, Frontoparietal R-Lateral Visual/Parietal, Frontoparietal R-Auditory/language, and Auditory/language-Frontoparietal L, Fig. 5a, Table. 2). Fig. 5b and 5c showed the yearly growth of the 14 network-level connectivity decreases (overall connectivity decreases during the first two years of life ranging from −0.02 to −0.64) and 5 network-level connectivity increases (overall connectivity increases during the first two years of life ranging from 0.05 to 0.18), respectively. For network-level decreases, those between primary networks were among the fastest decreasing ones (1st, 2nd, and 5th, Fig. 5b). All within- and between-network changes in functional connectivity were summarized in Table. 2. For both the intra- and inter-network connectivity growth, highly consistent results were observed when either using more stringent motion correction thresholds or adopting no global signal regression (Fig. S3, S4, Table S3)

Significant sex and growth rate interactions were detected for one inter-network connection: the rate of age-dependent increase in connectivity between the two frontoparietal components was greater in boys than girls (growth rate was 1.63e-4 and 2.69e-4 per day for girls and boys, respectively, $p<1e-4$ for the gender*growth rate interaction, Fig. 6). No significant gender effect was observed for any other between-network or within-network connections.

DISCUSSION

In this study, we delineated the development of the whole brain functional network architecture during the first two years of life based on longitudinal modeling of a large cohort of infants (n=143) with multiple scans. Our results show that local connectivity and bilateral symmetric functional connectivity emerge in neonates forming adult-like primary visual and motor-sensory networks. However, higher-order functional networks experience dramatic long-range synchronization postnatally. For inter-network interactions, network-level connectivity decreases dominate network-level connectivity increases. Finally, significant sex differences were observed for the integration between the two components of the frontoparietal network (boys faster than girls).

Consistent with our findings of adult-like visual and sensorimotor networks *at birth*, the prenatal development of visual and sensorimotor functions was well documented (Prechtl 1989; Kostovic et al. 1995; Doria et al. 2011). Bilateral symmetric connectivity between early visual and pre-/post-central areas was observed prenatally (Doria et al. 2011; Smyser et al. 2010). The early synchronization of these two primary networks (Lin et al. 2008) and proper functioning of corresponding skills may be evolutionally optimized to ensure early survival. Interestingly, the interaction between the two visual components shows a linear specialization trend during the first two years of life (Fig. 5). Similarly, the connectivity within the sensorimotor network also experienced age-dependent decreases during this time (Fig. 4). Such reduction in connectivity strength may represent functional specialization and a trend towards more efficient interaction patterns in primary functional areas (Tau and Peterson 2010).

The first year of life witnesses impressive increases in within-network functional connections (Fig. 4), which is highly consistent with the qualitative emergence of distributred network structures shown in Fig. 1. Previously, we have shown the synchronization process for the default-mode (Gao et al. 2009) and dorsal attention network (Gao et al. 2012), respectively. In this study, we extended such findings to all major networks that are observed in adults including the lateral visual/parietal, the auditory/language, the salience and the frontoparietal networks. Behaviorally, the dramatic synchronization process of these higher order cognitive networks corresponds well with the fast improvement in spatial attention (Haith et al. 1988; Rothbart and Posner 2001), language (Conboy et al. 2008), social awareness(Amsterdam 1972; Field 1979), and other higher-order brain functions(Posner and Rothbart 1998; Rothbart 1990) during this period. However, future studies directly linking functional connectivity development and behavioral measures are needed to validate their relationships. Overall, findings in this study suggest that the first year of life is a critical period for the establishment of various spatially distributed functional networks (Tau and Peterson 2010).

In contrast to within-network synchronization, wide-spread inter-network connectivity decreases were observed during the first two years of life. Specifically, 14 network-level interactions decrease while only 4 of them show increases (Fig. 5). Among them, the fastest decrease of connectivity between primary visual and sensorimotor networks likely indicates an increasing level of functional segregation between the two sensory modalities (Fig. 5). The largest portion of network-level connectivity decreases was between primary networks and associative ones (9 out of 16, Fig. 5) likely indicating emerging specializations between primary and higher-order cognitive functions during early development. The three decreasing network-level interactions among higher-order cognitive networks also agree with the dissociable functional roles between the default-mode and lateral visual/parietal network (Raichle et al. 2001; Buckner et al. 2008), between the default-mode and salience network (Seeley et al. 2007; Gao and Lin 2012), as well as between the salience and frontoparietal network (Seeley et al. 2007). Particularly, the lateral visual/parietal network in this study resembles the dorsal attention network in its topology and the early functional segregation between this network and the default-mode network has been reported in one of our previous studies (Gao et al. 2012). Since the dorsal attention network is mainly active in external attention tasks (Corbetta and Shulman 2002) while the default-mode network is

mainly involved in self-related internal thinking process (Buckner et al. 2008; Gusnard et al. 2001; Raichle et al. 2001; Shulman et al. 1997; Fox et al. 2005), the early segregation of this pair of networks is intriguing and coincides with behavioral observations of the competing external attention processes (i.e., focusing attention to a new toy) and internal stress states (i.e., crying) during the first year of life (Harman et al. 1997; Rothbart and Posner 2001). Taken together, the observed inter-network connectivity decreases are consistent with the functional segregation pattern of the adult brain supporting the notion that during this early brain developmental period different networks are not only establishing their within-network coordination but also establishing increasingly adult-like between-network segregation patterns. Among the five network-level connectivity increases, two were between the auditory/language network and the frontoparietal components. This increasing level of coordination may reflect an increasing need for cognitive control over the language-related processes which are quickly developing during this period of time (Conboy et al. 2008). Given the close relationship between the two frontoparietal components, the increasing integration between them may represent improving coordination within the large system (Vincent et al. 2008). The increasing connectivity between the default mode network and the right frontoparietal network during the sleeping state in this study is less intuitive since heightened interaction of these two components is typically observed with elevated levels of cognitive demands (Gao and Lin 2012; Spreng et al. 2010; Elton and Gao In Press; Gao et al. 2013). However, the developmental significance of this interaction likely differs from its adult roles (Johnson 2000) and needs further investigation.

Finally, the significant sex differences observed for the inter-network connectivity development are intriguing. Specifically, boys demonstrated faster integration of the two frontoparietal components compared with girls. Given the clear executive control role of the frontoparietal network in complex external goal-directed tasks (Seeley et al. 2007; Vincent et al. 2008), this finding might suggest boys would gain developmental advantage along this line of behaviors during development, which may find certain support from previous behavioral findings (Busch 1995; Chai and Jacobs 2009). Overall, successful detection of sex differences on network-level functional connectivity in this study suggest that resting-state fMRI could be used as an effective means for delineating the brain basis of sex-related behavior differences in a developmental setting.

Technical Considerations

To explore the whole brain functional network architecture, the data-driven ICA approach was adopted in this study to objectively define all possible functional networks for each age group. In contrast to seed-based analysis which is only capable of delineating specific functional networks based on pre-defined seed regions, ICA is able to simultaneously unveil all possible network structures within the brain by maximizing temporal similarity within components and spatial independence among components (Calhoun et al. 2001). Therefore, ICA is deemed to be better suited for this study which aims to objectively evaluate the emergence of all potential functional networks during early brain development. However, there are recognized difficulties in the functional interpretation of the components derived from ICA and a commonly accepted approach to alleviate such difficulties is to spatially match ICA components to known functional networks to ease the interpretation (Gao et al.

2009; Greicius et al. 2004). Therefore, with the aim to delineate how adult-like functional networks emerge during infancy, we chose to use the nine cortical networks defined in Smith et al (2009) as reference networks to spatially match the ICA components derived from each individual age groups to facilitate our interpretation of the development of cortical networks.

Several other technical issues deserve further discussion. First, the definition of functional regions was based on a “winner-takes-all” approach using the derived ICA components. This approach was used to define spatially non-overlapping regions since overlapping regions in ICA components, which occur frequently, may contaminate the connectivity estimate between different functional networks. In the future, the application of more sophisticated functional parcellation approach (Craddock et al. 2012) within ICA-defined large regions may be beneficial to define smaller sub-regions and better remove overlapping between different components. Secondly, in the spatial matching process, although a relatively low threshold (0.2) was used visual inspection has confirmed spatial correspondence between infant and adult ICA maps. Moreover, the temporal growth patterns of both the within- and between-network connections were highly similar when directly using the adult maps to define the functional regions indicating the effectiveness of this spatial matching. Thirdly, we performed global signal regression in our preprocessing to control for physiological noise instead of applying external monitoring devices primarily because of the great challenge associated with applying these devices to sleeping infants. Chang and Glover (Chang and Glover 2009) showed a high correspondence between the global signal and the externally monitored respiratory and cardiac signals. Therefore, it is highly plausible that such physiological confounds have been substantially minimized using this regression approach(Power et al. 2014). Moreover, we tried to focus our discussion on the relative changes of functional connectivity. Indeed, direct comparisons of the growth curves for both within- and between-network connectivity show highly consistent results between data with and without global signal regression (Fig. S3, S4, Table S3). Additionally, although ICA has the capability to separate artifact signals, it was applied on standard preprocessed images in this study with an aim to maximize its power in separating relevant signals into functionally meaningful functional networks rather than separating noise signals. Finally, regarding the motion artifacts, we have implemented the “scrubbing” method (Power et al. 2012a) to further reduce potential motion contamination after spatial re-alignment. Given the recent suggestions of a more stringent threshold (Power et al. 2012b) (frame-wise displacement <0.2 mm and signal intensity change <0.3%) comparing with the one used in the main analyses (frame-wise displacement <0.5 mm or signal intensity change <0.5%), we have provided results comparing the two scrubbing thresholds and again highly consistent results were obtained (Fig. S3, S4, Table S3).

Conclusion

In this study, we have documented the emergence of the whole-brain network structure during the first two years of life. Using a data-driven independent component analysis (ICA) approach, pediatric brains rsfMRI data were decomposed into individual functional networks and matched with those in adults. A local-to-distributed pattern was observed for most higher-order cognitive networks in which neonates featured isolated local connectivity while distributed network structures developed postnatally, especially during the first year of

life. Besides within-network synchronization, different networks are also establishing increasingly adult-like between-network interaction patterns featuring more dramatic network-level connectivity decreases than increases. More importantly, interesting sex differences also emerge during this process. The delineation of the functional network development of the healthy brain during the first two years of life may provide critical reference for future investigations into different developmental disorders.

Supplementary Material

Refer to Web version on PubMed Central for supplementary material.

Acknowledgments

This work was supported by National Institutes of Health grant R01MH070890-09A1 to JHG; R01NS055754 to WL; Foundation *of Hope for Research and Treatment of Mental Illness* Award to WG; and UNC-Chapel Hill startup fund to WG.

References

Alcauter S, Lin W, Smith JK, Gilmore JH, Gao W. Consistent Anterior-Posterior Segregation of the Insula during the First Two Years of Life. Cerebral Cortex. 201310.1093/cercor/bht1312

Amsterdam B. Mirror self-image reactions before age two. Developmental Psychology. Psychology. 1972; 5(4):297–305.

Andrews-Hanna JR, Snyder AZ, Vincent JL, Lustig C, Head D, Raichle ME, Buckner RL. Disruption of large-scale brain systems in advanced aging. Neuron. 2007; 56(5):924–935.10.1016/j.neuron.2007.10.038 [PubMed: 18054866]

Biswal B, Yetkin FZ, Haughton VM, Hyde JS. Functional connectivity in the motor cortex of resting human brain using echo-planar MRI. Magn Reson Med. 1995; 34(4):537–541. [PubMed: 8524021]

Buckner RL, Andrews-Hanna JR, Schacter DL. The brain's default network: anatomy, function, and relevance to disease. Ann N Y Acad Sci. 2008; 1124:1–38. 1124/1/1 [pii]. 10.1196/annals.1440.011 [PubMed: 18400922]

Buckner RL, Krienen FM, Castellanos A, Diaz JC, Yeo BT. The organization of the human cerebellum estimated by intrinsic functional connectivity. J Neurophysiol. 2011; 106(5):2322–2345.10.1152/jn.00339.2011 [PubMed: 21795627]

Busch T. Gender differences in self-efficacy and attitudes toward computers. Journal of Educational Computing Research. 1995; 12:147–158.

Calhoun VD, Adali T, Pearlson GD, Pekar JJ. A method for making group inferences from functional MRI data using independent component analysis. Hum Brain Mapp. 2001; 14(3):140–151. pii. 10.1002/hbm.1048 [PubMed: 11559959]

Chai XJ, Jacobs LF. Sex differences in directional cue use in a virtual landscape. Behav Neurosci. 2009; 123(2):276–283.10.1037/a0014722 [PubMed: 19331451]

Chang C, Glover GH. Effects of model-based physiological noise correction on default mode network anti-correlations and correlations. Neuroimage. 2009; 47(4):1448–1459. S1053-8119(09)00512-6 [pii]. 10.1016/j.neuroimage.2009.05.012 [PubMed: 19446646]

Conboy BT, Sommerville JA, Kuhl PK. Cognitive control factors in speech perception at 11 months. Dev Psychol. 2008; 44(5):1505–1512.10.1037/a0012975 [PubMed: 18793082]

Corbetta M, Shulman GL. Control of goal-directed and stimulus-driven attention in the brain. Nat Rev Neurosci. 2002; 3(3):201–215.10.1038/nrn755 [PubMed: 11994752]

Craddock RC, James GA, Holtzheimer PE 3rd, Hu XP, Mayberg HS. A whole brain fMRI atlas generated via spatially constrained spectral clustering. Hum Brain Mapp. 2012; 33(8):1914–1928.10.1002/hbm.21333 [PubMed: 21769991]

Damoiseaux JS, Rombouts SA, Barkhof F, Scheltens P, Stam CJ, Smith SM, Beckmann CF. Consistent resting-state networks across healthy subjects. Proc Natl Acad Sci U S A. 2006; 103(37):13848–13853. 0601417103 [pii]. 10.1073/pnas.0601417103 [PubMed: 16945915]

Di Martino A, Kelly C, Grzadzinski R, Zuo XN, Mennes M, Mairena MA, Lord C, Castellanos FX, Milham MP. Aberrant striatal functional connectivity in children with autism. Biol Psychiatry. 2010; 69(9):847–856. S0006-3223(10)01162-5 [pii]. 10.1016/j.biopsych.2010.10.029 [PubMed: 21195388]

Dickstein DP, Gorrostieta C, Ombao H, Goldberg LD, Brazel AC, Gable CJ, Kelly C, Gee DG, Zuo XN, Castellanos FX, Milham MP. Fronto-temporal spontaneous resting state functional connectivity in pediatric bipolar disorder. Biol Psychiatry. 2010; 68(9):839–846. S0006-3223(10)00710-9 [pii]. 10.1016/j.biopsych.2010.06.029 [PubMed: 20739018]

Doria V, Beckmann CF, Arichi T, Merchant N, Groppo M, Turkheimer FE, Counsell SJ, Murgasova M, Aljabar P, Nunes RG, Larkman DJ, Rees G, Edwards AD. Emergence of resting state networks in the preterm human brain. Proc Natl Acad Sci U S A. 2011; 107(46):20015–20020. 1007921107 [pii]. 10.1073/pnas.1007921107 [PubMed: 21041625]

Ebbels TM, Buxton BF, Jones DT. springScape: visualisation of microarray and contextual bioinformatic data using spring embedding and an ‘information landscape’. Bioinformatics. 2006; 22(14):e99–107. 22/14/e99 [pii]. 10.1093/bioinformatics/btl205 [PubMed: 16873528]

Elton A, Gao W. Divergent Task-Dependent Functional Connectivity of Executive Control and Salience Networks. Cortex; a journal devoted to the study of the nervous system and behavior. In Press.

Fair DA, Cohen AL, Dosenbach NU, Church JA, Miezin FM, Barch DM, Raichle ME, Petersen SE, Schlaggar BL. The maturing architecture of the brain’s default network. Proc Natl Acad Sci U S A. 2008; 105(10):4028–4032. 0800376105 [pii]. 10.1073/pnas.0800376105 [PubMed: 18322013]

Fair DA, Cohen AL, Power JD, Dosenbach NU, Church JA, Miezin FM, Schlaggar BL, Petersen SE. Functional brain networks develop from a “local to distributed” organization. PLoS Comput Biol. 2009; 5(5):e1000381.10.1371/journal.pcbi.1000381 [PubMed: 19412534]

Fair DA, Posner J, Nagel BJ, Bathula D, Dias TG, Mills KL, Blythe MS, Giwa A, Schmitt CF, Nigg JT. Atypical default network connectivity in youth with attention-deficit/hyperactivity disorder. Biol Psychiatry. 2010; 68(12):1084–1091. S0006-3223(10)00706-7 [pii]. 10.1016/j.biopsych.2010.07.003 [PubMed: 20728873]

Field T. Differential behavioral and cardiac responses of 3-month-old infants to a mirror and peer. Infant Behavior & Development. 1979; 2:179–184.

Fornito A, Harrison BJ, Zalesky A, Simons JS. Competitive and cooperative dynamics of large-scale brain functional networks supporting recollection. Proc Natl Acad Sci U S A. 2012; 109(31):12788–12793.10.1073/pnas.1204185109 [PubMed: 22807481]

Fox MD, Snyder AZ, Vincent JL, Corbetta M, Van Essen DC, Raichle ME. The human brain is intrinsically organized into dynamic, anticorrelated functional networks. Proc Natl Acad Sci U S A. 2005; 102(27):9673–9678. 0504136102 [pii]. 10.1073/pnas.0504136102 [PubMed: 15976020]

Fransson P, Skiold B, Horsch S, Nordell A, Blennow M, Lagercrantz H, Aden U. Resting-state networks in the infant brain. Proc Natl Acad Sci U S A. 2007; 104(39):15531–15536.10.1073/pnas.0704380104 [PubMed: 17878310]

Friston KJ, Frith CD, Liddle PF, Frackowiak RS. Functional connectivity: the principal-component analysis of large (PET) data sets. J Cereb Blood Flow Metab. 1993; 13(1):5–14. [PubMed: 8417010]

Gao W, Gilmore JH, Alcauter S, Lin W. The dynamic reorganization of the default-mode network during a visual classification task. Front Syst Neurosci. 2013; 7:34.10.3389/fnsys.2013.00034 [PubMed: 23898240]

Gao W, Gilmore JH, Giovanello KS, Smith JK, Shen D, Zhu H, Lin W. Temporal and spatial evolution of brain network topology during the first two years of life. PLoS One. 2011; 6(9):e25278.10.1371/journal.pone.0025278 [PubMed: 21966479]

Gao W, Gilmore JH, Shen D, Smith JK, Zhu H, Lin W. The Synchronization within and Interaction between the Default and Dorsal Attention Networks in Early Infancy. Cereb Cortex. 201210.1093/cercor/bhs1043

Gao W, Lin W. Frontal parietal control network regulates the anti-correlated default and dorsal attention networks. Hum Brain Mapp. 2012; 33(1):192–202.10.1002/hbm.21204 [PubMed: 21391263]

Gao W, Zhu H, Giovanello KS, Smith JK, Shen D, Gilmore JH, Lin W. Evidence on the emergence of the brain's default network from 2-week-old to 2-year-old healthy pediatric subjects. Proc Natl Acad Sci U S A. 2009; 106(16):6790–6795.10.1073/pnas.0811221106 [PubMed: 19351894]

Gaulin, S. The Development of Sex Differences and Similarities in Behavior. Kluwer Academic Publisher; Gers, France: 1993. How and Why Sex Differences Evolve, with Spatial Ability as a Paradigm Example.

Gilmore JH, Shi F, Woolson SL, Knickmeyer RC, Short SJ, Lin W, Zhu H, Hamer RM, Styner M, Shen D. Longitudinal Development of Cortical and Subcortical Gray Matter from Birth to 2 Years. Cereb Cortex. 2012 bhr327 [pii]. 10.1093/cercor/bhr327

Greicius MD, Srivastava G, Reiss AL, Menon V. Default-mode network activity distinguishes Alzheimer's disease from healthy aging: evidence from functional MRI. Proc Natl Acad Sci U S A. 2004; 101(13):4637–4642. 0308627101 [pii]. 10.1073/pnas.0308627101 [PubMed: 15070770]

Gusnard DA, Akbudak E, Shulman GL, Raichle ME. Medial prefrontal cortex and self-referential mental activity: relation to a default mode of brain function. Proc Natl Acad Sci U S A. 2001; 98(7):4259–4264.10.1073/pnas.071043098 [PubMed: 11259662]

Haith MM, Hazan C, Goodman GS. Expectation and anticipation of dynamic visual events by 3.5-month-old babies. Child Dev. 1988; 59(2):467–479. [PubMed: 3359865]

Harman C, Rothbart MK, Posner MI. Distress and attention interactions in early infancy. Motiv Emot. 1997; 21:27–43.

Johnson MH. Functional brain development in infants: elements of an interactive specialization framework. Child Dev. 2000; 71(1):75–81. [PubMed: 10836560]

Kail, M. The Development of Sex Differences and Similarities in Behavior. Kluwer Academic Publisher; Gers, France: 1993. Are Sex or Gender Relevant Categories to Language Performance? A Critical Review.

Kelly AM, Di Martino A, Uddin LQ, Shehzad Z, Gee DG, Reiss PT, Margulies DS, Castellanos FX, Milham MP. Development of anterior cingulate functional connectivity from late childhood to early adulthood. Cereb Cortex. 2009; 19(3):640–657. bhn117 [pii]. 10.1093/cercor/bhn117 [PubMed: 18653667]

Kilpatrick LA, Zald DH, Pardo JV, Cahill LF. Sex-related differences in amygdala functional connectivity during resting conditions. Neuroimage. 2006; 30(2):452–461.10.1016/j.neuroimage.2005.09.065 [PubMed: 16326115]

Kostovic I, Judas M, Petanjek Z, Simic G. Ontogenesis of goal-directed behavior: anatomo-functional considerations. Int J Psychophysiol. 1995; 19(2):85–102. [PubMed: 7622411]

Lin W, Zhu Q, Gao W, Chen Y, Toh CH, Styner M, Gerig G, Smith JK, Biswal B, Gilmore JH. Functional connectivity MR imaging reveals cortical functional connectivity in the developing brain. AJNR Am J Neuroradiol. 2008; 29(10):1883–1889.10.3174/ajnr.A1256 [PubMed: 18784212]

Posner MI, Rothbart MK. Attention, self-regulation and consciousness. Philos Trans R Soc Lond B Biol Sci. 1998; 353(1377):1915–1927.10.1098/rstb.1998.0344 [PubMed: 9854264]

Power JD, Barnes KA, Snyder AZ, Schlaggar BL, Petersen SE. Spurious but systematic correlations in functional connectivity MRI networks arise from subject motion. Neuroimage. 2012a; 59(3):2142–2154.10.1016/j.neuroimage.2011.10.018 [PubMed: 22019881]

Power JD, Barnes KA, Snyder AZ, Schlaggar BL, Petersen SE. Steps toward optimizing motion artifact removal in functional connectivity MRI; a reply to Carp. Neuroimage. 2012b10.1016/j.neuroimage.2012.03.017

Power JD, Barnes KA, Snyder AZ, Schlaggar BL, Petersen SE. Steps toward optimizing motion artifact removal in functional connectivity MRI; a reply to Carp. Neuroimage. 2013; 76:439–441.10.1016/j.neuroimage.2012.03.017 [PubMed: 22440651]

Power JD, Fair DA, Schlaggar BL, Petersen SE. The development of human functional brain networks. Neuron. 2010; 67(5):735–748.10.1016/j.neuron.2010.08.017 [PubMed: 20826306]

Power JD, Mitra A, Laumann TO, Snyder AZ, Schlaggar BL, Petersen SE. Methods to detect, characterize, and remove motion artifact in resting state fMRI. Neuroimage. 2014; 84:320–341.10.1016/j.neuroimage.2013.08.048 [PubMed: 23994314]

Prechtl, HFR. Fetal Neurology. Raven Press; New York: 1989. Fetal Behavior.

Raichle ME, MacLeod AM, Snyder AZ, Powers WJ, Gusnard DA, Shulman GL. A default mode of brain function. Proc Natl Acad Sci U S A. 2001; 98(2):676–682.10.1073/pnas.98.2.676 [PubMed: 11209064]

Rombouts SA, Barkhof F, Goekoop R, Stam CJ, Scheltens P. Altered resting state networks in mild cognitive impairment and mild Alzheimer's disease: an fMRI study. Hum Brain Mapp. 2005; 26(4):231–239.10.1002/hbm.20160 [PubMed: 15954139]

Rothbart, MK. Regulatory mechanisms in infant development The development of attention: Research and Theory. Elsevier/North-Holland; Amstardam: 1990.

Rothbart, MK.; Posner, MI. Handbook of developmental cognitive neuroscience. MIT Press; Cambridge: 2001. Mechanism and Variation in the Development of Attentional Networks.

Satterthwaite TD, Elliott MA, Gerraty RT, Ruparel K, Loughead J, Calkins ME, Eickhoff SB, Hakonarson H, Gur RC, Gur RE, Wolf DH. An improved framework for confound regression and filtering for control of motion artifact in the preprocessing of resting-state functional connectivity data. Neuroimage. 2013; 64:240–256.10.1016/j.neuroimage.2012.08.052 [PubMed: 22926292]

Satterthwaite TD, Wolf DH, Loughead J, Ruparel K, Elliott MA, Hakonarson H, Gur RC, Gur RE. Impact of in-scanner head motion on multiple measures of functional connectivity: relevance for studies of neurodevelopment in youth. Neuroimage. 2012; 60(1):623–632.10.1016/j.neuroimage.2011.12.063 [PubMed: 22233733]

Seeley WW, Menon V, Schatzberg AF, Keller J, Glover GH, Kenna H, Reiss AL, Greicius MD. Dissociable intrinsic connectivity networks for salience processing and executive control. J Neurosci. 2007; 27(9):2349–2356.10.1523/JNEUROSCI.5587-06.2007 [PubMed: 17329432]

Shen D, Davatzikos C. Measuring temporal morphological changes robustly in brain MR images via 4-dimensional template warping. Neuroimage. 2004; 21(4):1508–1517. S1053811903007808 [pii]. 10.1016/j.neuroimage.2003.12.015 [PubMed: 15050575]

Shi F, Yap PT, Wu G, Jia H, Gilmore JH, Lin W, Shen D. Infant brain atlases from neonates to 1- and 2-year-olds. PLoS One. 2011; 6(4):e18746.10.1371/journal.pone.0018746 [PubMed: 21533194]

Shulman G, Fiez J, Corbetta M, Buckner R, Miezin F. Common blood flow changes across visual tasks: II. Decreases in cerebral cortex. J Cogn Neurosci. 1997; 9:648–663. [PubMed: 23965122]

Smith SM, Fox PT, Miller KL, Glahn DC, Fox PM, Mackay CE, Filippini N, Watkins KE, Toro R, Laird AR, Beckmann CF. Correspondence of the brain's functional architecture during activation and rest. Proc Natl Acad Sci U S A. 2009; 106(31):13040–13045.10.1073/pnas.0905267106 [PubMed: 19620724]

Smith SM, Jenkinson M, Woolrich MW, Beckmann CF, Behrens TE, Johansen-Berg H, Bannister PR, De Luca M, Drobnjak I, Flitney DE, Niazy RK, Saunders J, Vickers J, Zhang Y, De Stefano N, Brady JM, Matthews PM. Advances in functional and structural MR image analysis and implementation as FSL. Neuroimage. 2004; 23(Suppl 1):S208–219.10.1016/j.neuroimage.2004.07.051 [PubMed: 15501092]

Smyser CD, Inder TE, Shimony JS, Hill JE, Degnan AJ, Snyder AZ, Neil JJ. Longitudinal Analysis of Neural Network Development in Preterm Infants. Cereb Cortex. 2010 bhq035 [pii]. 10.1093/cercor/bhq035

Spreng RN, Stevens WD, Chamberlain JP, Gilmore AW, Schacter DL. Default network activity, coupled with the frontoparietal control network, supports goal-directed cognition. Neuroimage. 2010; 53(1):303–317. S1053-8119(10)00860-8 [pii]. 10.1016/j.neuroimage.2010.06.016 [PubMed: 20600998]

Sripada RK, King AP, Welsh RC, Garfinkel SN, Wang X, Sripada CS, Liberzon I. Neural dysregulation in posttraumatic stress disorder: evidence for disrupted equilibrium between salience and default mode brain networks. Psychosom Med. 2012; 74(9):904–911.10.1097/PSY.0b013e318273bf33 [PubMed: 23115342]

Stern ER, Fitzgerald KD, Welsh RC, Abelson JL, Taylor SF. Resting-state functional connectivity between fronto-parietal and default mode networks in obsessive-compulsive disorder. PLoS One. 2012; 7(5):e36356.10.1371/journal.pone.0036356 [PubMed: 22570705]

Supekar K, Musen M, Menon V. Development of large-scale functional brain networks in children. PLoS Biol. 2009; 7(7):e1000157.10.1371/journal.pbio.1000157 [PubMed: 19621066]

Tau GZ, Peterson BS. Normal development of brain circuits. Neuropsychopharmacology. 2010; 35(1): 147–168. npp2009115 [pii]. 10.1038/npp.2009.115 [PubMed: 19794405]

Tomasi D, Volkow ND. Gender differences in brain functional connectivity density. Hum Brain Mapp. 2012; 33(4):849–860.10.1002/hbm.21252 [PubMed: 21425398]

Vincent JL, Kahn I, Snyder AZ, Raichle ME, Buckner RL. Evidence for a frontoparietal control system revealed by intrinsic functional connectivity. J Neurophysiol. 2008; 100(6):3328–3342. 90355.2008 [pii]. 10.1152/jn.90355.2008 [PubMed: 18799601]

Wang J, Zuo X, Dai Z, Xia M, Zhao Z, Zhao X, Jia J, Han Y, He Y. Disrupted Functional Brain Connectome in Individuals at Risk for Alzheimer's Disease. Biol Psychiatry. 201210.1016/j.biopsych.2012.03.026

Yeo BT, Krienen FM, Sepulcre J, Sabuncu MR, Lashkari D, Hollinshead M, Roffman JL, Smoller JW, Zollei L, Polimeni JR, Fischl B, Liu H, Buckner RL. The organization of the human cerebral cortex estimated by intrinsic functional connectivity. J Neurophysiol. 2011; 106(3):1125–1165.10.1152/jn.00338.2011 [PubMed: 21653723]

Zhang D, Snyder AZ, Fox MD, Sansbury MW, Shimony JS, Raichle ME. Intrinsic functional relations between human cerebral cortex and thalamus. J Neurophysiol. 2008; 100(4):1740–1748.10.1152/jn.90463.2008 [PubMed: 18701759]

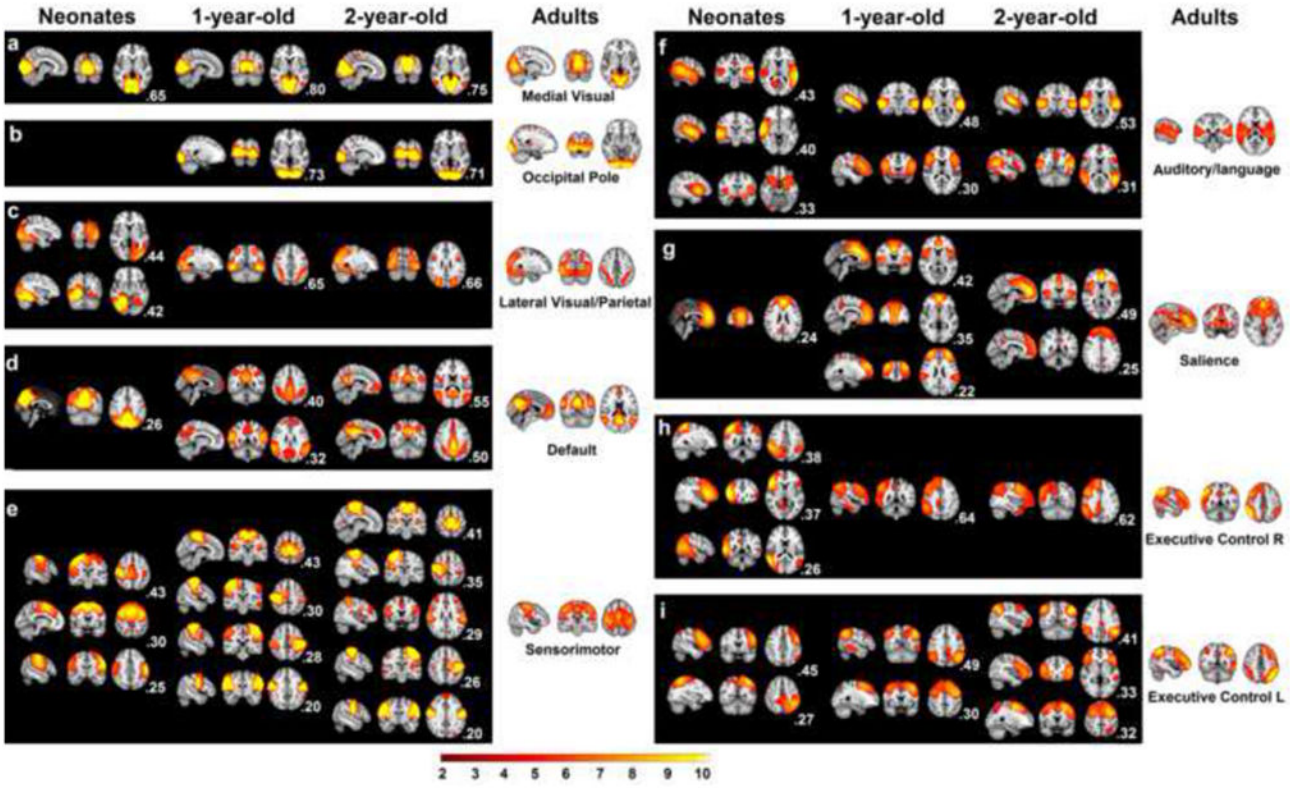

Figure 1.

Functional networks derived from ICA for three infant groups. Only those with a spatial correspondence with one of 9 adult networks are shown. The spatial correlation value of each ICA map with the corresponding adult network map is shown at the right bottom of each panel. For each panel, three orthogonal brain images are used to represent the spatial topology of corresponding ICA maps (radiological convention: left image is right side of brain). a: the medial visual network; b: the occipital pole network; c: the lateral visual/ parietal network; d; the default-mode network; e: the sensorimotor network; f: the auditory/ language network; g: the salience network; h: the right Frontoparietal network; i: the left Frontoparietal network. All maps were thresholded at Z>2.

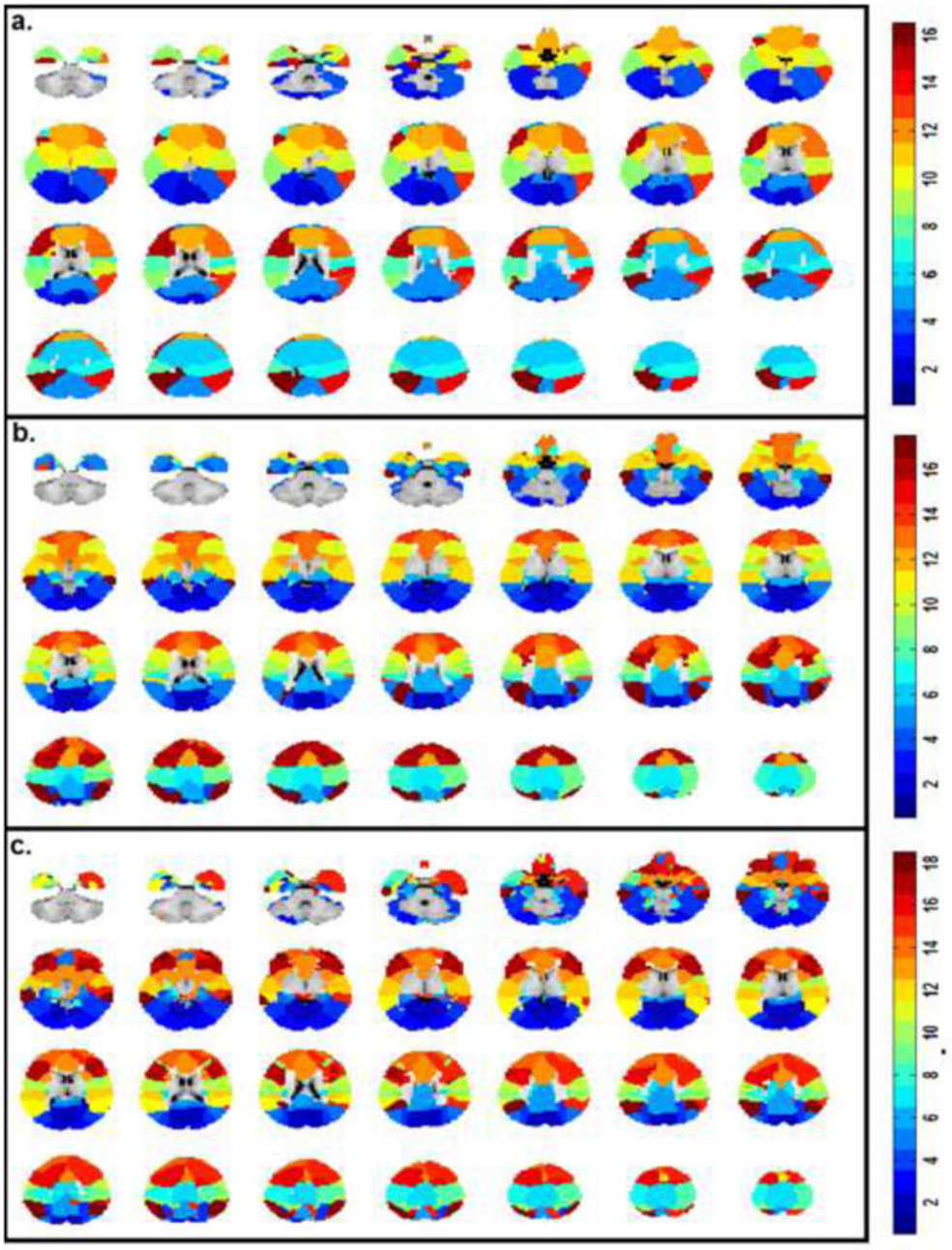

Figure 2.

Functional parcellation of the brain in infants using a “winner-takes-all” approach based on the age-specific ICA components. a. Neonates; b. one-year olds; c. two-year olds. Color bars represent the different ICA components that each functionally parcellated region belongs to (i.e., 16, 17, and 18 for neonates, one-year olds and two-year olds, respectively).

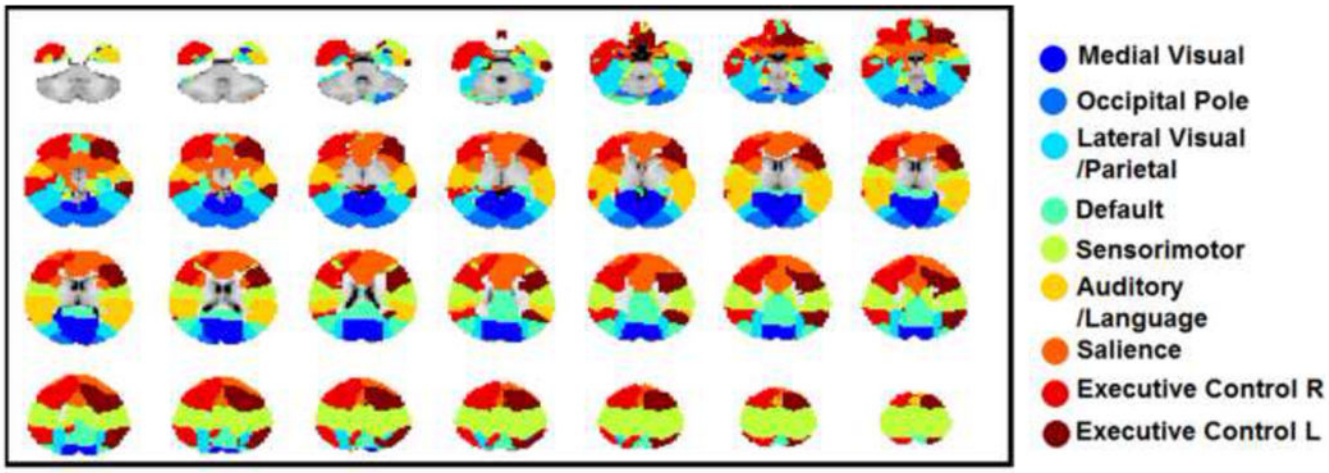

Figure 3.
Network-level parcellation of the cerebral cortex in two-year olds guided by the nine adult networks.

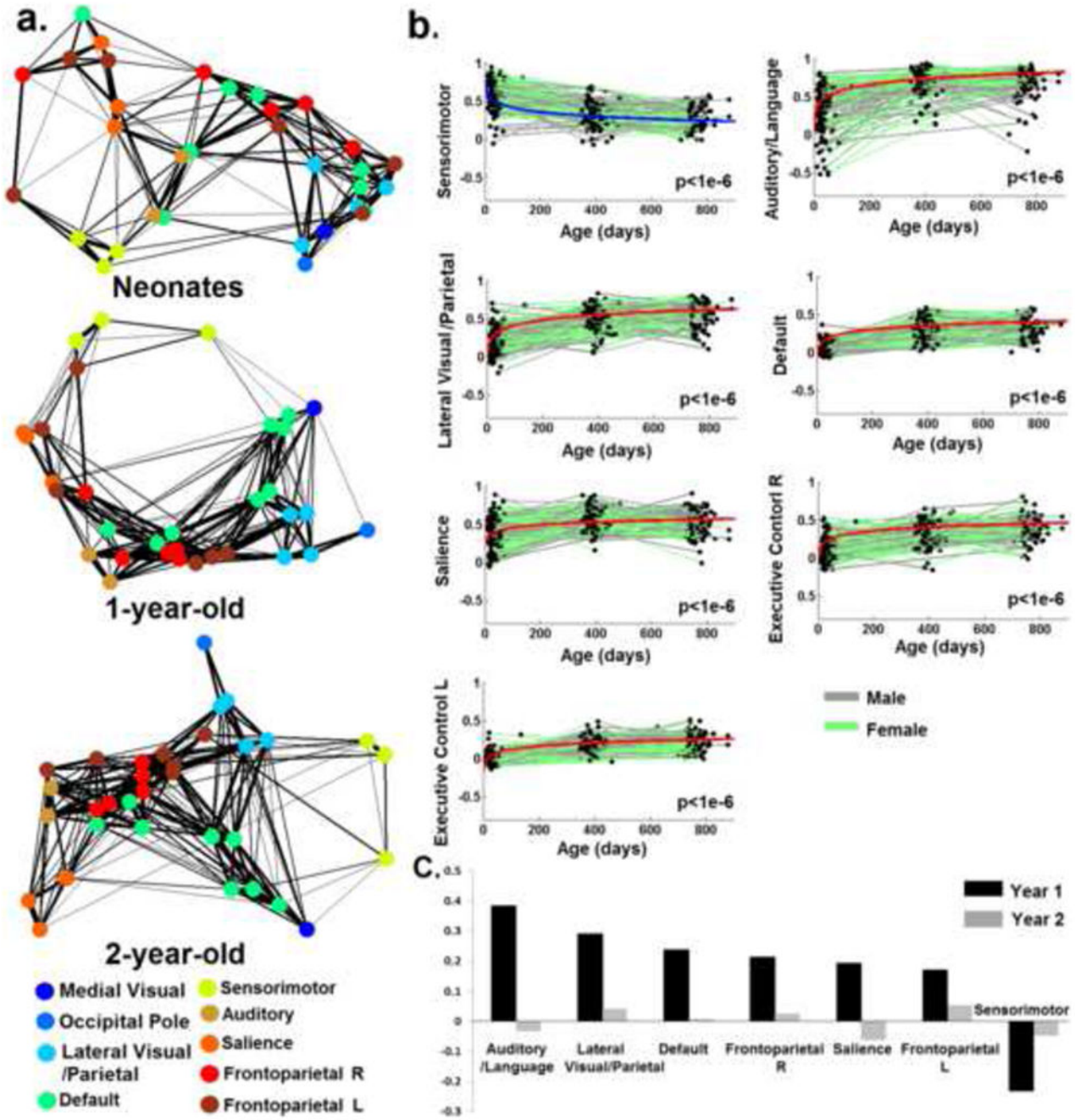

Figure 4.

The development of within-network functional connectivity. a). Spring-embedding plots showing the development of the connectivity pattern of 33 functionally-defined regions based on 2-year-olds data. Regions belonging to the same network (Fig. 3) were labeled the same color; b). Longitudinal growth trajectory of the mean connectivity within each network. The group-mean growth model of each network represented by the fixed effect parameters is plotted on top of the “spaghetti” plot of functional connectivity changes observed in individual subjects. Males are shown in gray while females are shown in green.

Models featuring age-dependent decreases in connectivity are visualized in blue while those featuring age-dependent increases are visualized in red. P-values of each model (the growth term) are shown at the right bottom of each panel; c). Yearly growths of within-network functional connectivity in descending order according to Year 1 growth measurements. Note the medial visual and occipital pole networks were not included in b) and c) since only one region was defined for each of the networks and there was no inter-region within-network connection.

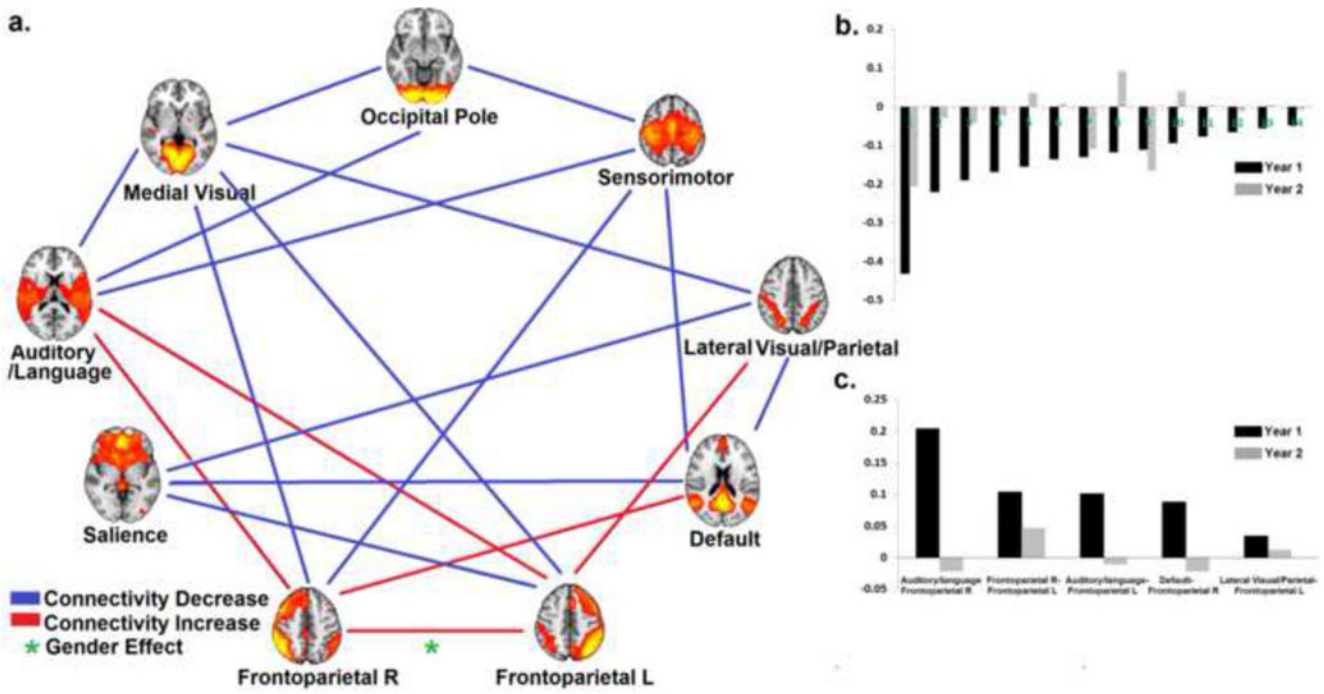

Figure 5.

a) Graph showing the age-dependent growth trend of inter-network connectivity. Network-level specializations (i.e., age-dependent decrease in connectivity) are shown in blue while network-level integrations (i.e., age-dependent increase in connectivity) are shown in red. Green asterisks represent significant sex differences ($p<0.05$ after FDR correction); b). Yearly growth of the 16 network-level specializations in descending order according to Year 1 growth measurements; 1. Medial Visual- Occipital Pole; 2. Medial Visual- Occipital Pole; 3. Medial Visual-Frontoparietal L; 4. Medial Visual-Auditory/language; 5. Occipital Pole-Sensorimotor; 6. Default-Sensorimotor; 7. Medial Visual-Frontoparietal R; 8. Occipital Pole-Auditory/language; 9. Medial Visual-Lateral Visual/Parietal;10. Sensorimotor-Frontoparietal R; 11. Default-Salience; 12. Lateral Visual/Parietal-Salience; 13. Salience-Frontoparietal L; 14. Lateral Visual/Parietal—Default; c). Yearly growth of the 4 network-level integrations in descending order according to Year 1 growth measurements.

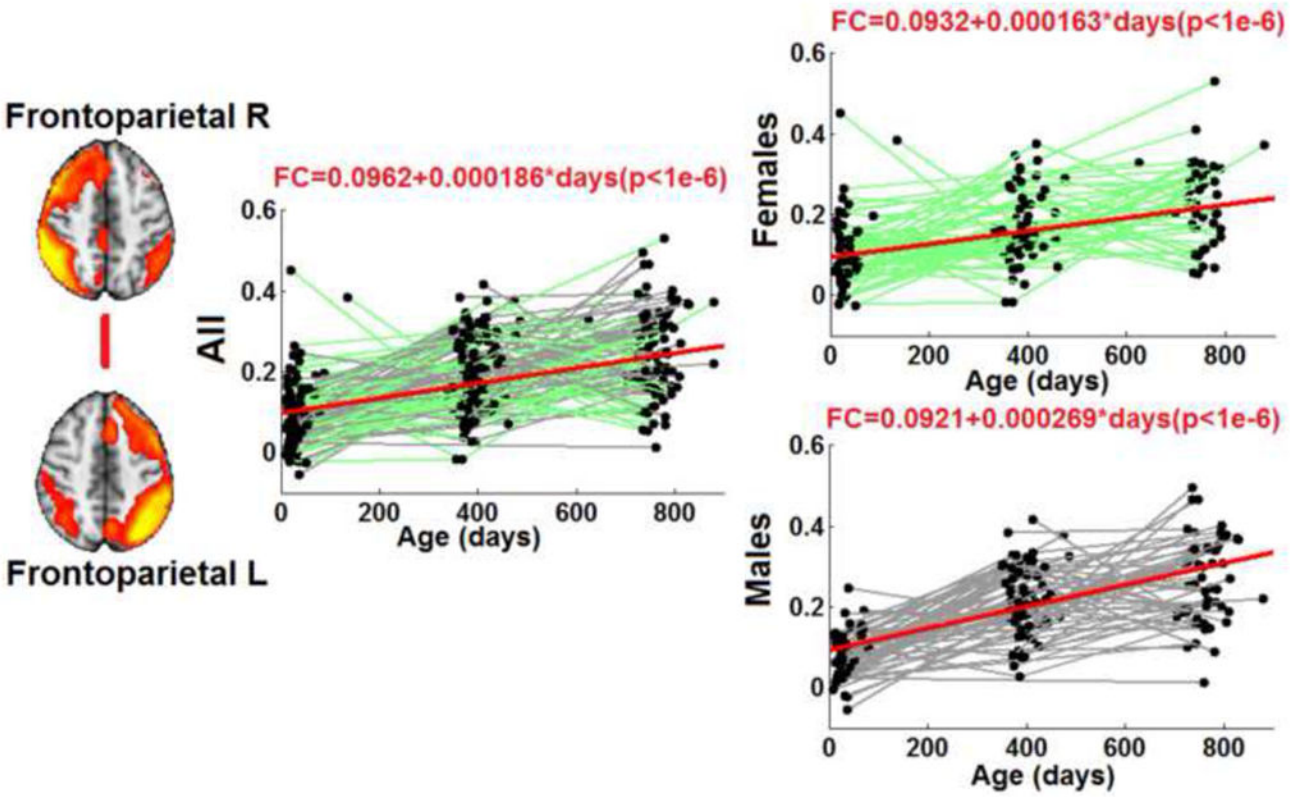

Figure 6.

Significant sex differences on the development of two network-level interactions. Top panel: network-level connectivity between the default network and the lateral visual/parietal network. Bottom panel: network-level connectivity between the two Frontoparietal network components. Both the full model and two separate models (i.e., males and females) are shown for each of the two network-level connections with the same setting as that in Fig. 3.

Table 1

Distribution of ages at which subjects were scanned

Ages at scan (years)	Number of subjects
0 and 1	51 (25 male)
0 and 2	14 (7 male)
1 and 2	31 (21 male)
0, 1 and 2	47 (24 male)
Total	143 (77 male)

Table 2

Development of all within- and between-network interactions during the first two years of life. All parameters were from linear-mixed effect modeling of corresponding functional connectivity measures. Only parameters from the better fitted model (either linear or log-linear, according to the AIC criterion) were presented. Statistically significant increasing connections with age are in bold, decreasing connections with age are in bold italics.

Network	Model	Intercept	Slope	P (Slope)	AIC (Linear)	AIC (Log-linear)
Lateral Visual/Parietal	**Log-linear**	**−0.0347**	**0.0986**	**1.12E-34**	**−194.39**	**−239.56**
Default	**Log-linear**	**−0.0776**	**0.0724**	**4.40E-38**	**−433.59**	**−484.86**
Sensorimotor	***Log-linear***	**0.7889**	**−0.0818**	**8.48E-29**	**−221.69**	**−254.55**
Auditory/language	**Log-linear**	**0.0675**	**0.1117**	**3.39E-26**	**45.54**	**0.06**
Salience	**Log-linear**	**0.2104**	**0.0532**	**4.33E-13**	**−155.28**	**−193.60**
Frontoparietal R	**Log-linear**	**−0.0183**	**0.0709**	**8.55E-25**	**−263.16**	**−296.99**
Frontoparietal L	**Log-linear**	**−0.1686**	**0.0631**	**2.92E-39**	**−561.93**	**−583.60**
Medial Visual- Occipital Pole	***Linear***	**0.2583**	**−0.0008**	**2.29E-41**	**36.65**	**48.10**
Medial Visual-Lateral Visual/Parietal	***Linear***	**0.1988**	**−0.0003**	**4.90E-18**	**−132.03**	**−118.38**
Medial Visual-Default	*Log-linear*	0.1481	−0.0124	3.44E-02	−307.60	−310.66
Medial Visual-Sensorimotor	*Log-linear*	−0.0854	−0.0094	2.44E-01	−85.62	−96.89
Medial Visual-Auditory/language	***Log-linear***	**0.0799**	**−0.0524**	**2.70E-08**	**22.13**	**11.18**
Medial Visual-Salience	Log-linear	−0.0655	−0.0148	5.59E-02	−99.81	−112.58
Medial Visual-Frontoparietal R	***Log-linear***	**0.1183**	**−0.0625**	**9.70E-16**	**−170.94**	**−174.35**
Medial Visual-Frontoparietal L	***Linear***	**−0.1358**	**−0.0003**	**5.51E-28**	**−435.61**	**−407.43**
Occipital Pole-Lateral Visual/Parietal	Linear	0.1839	−0.0001	7.20E-02	−190.97	−180.58
Occipital Pole-Default	Log-linear	−0.0183	−0.0039	4.50E-01	−374.87	−385.75
Occipital Pole-Sensorimotor	***Log-linear***	**−0.0037**	**−0.0413**	**2.16E-07**	**−103.52**	**−124.58**
Occipital Pole-Auditory/language	***Log-linear***	**0.0373**	**−0.0205**	**2.26E-03**	**5.91**	**−8.51**
Occipital Pole-Salience	Log-linear	−0.0488	−0.0071	3.72E-01	−70.14	−81.55
Occipital Pole-Frontoparietal R	Log-linear	−0.0417	0.0058	3.52E-01	−246.28	−254.26
Occipital Pole-Frontoparietal L	Log-linear	−0.0709	0.0035	4.60E-01	−447.30	−455.29
Lateral Visual/Parietal--Default	***Linear***	**0.0808**	**−0.0001**	**4.83E-04**	**−556.66**	**−545.31**
Lateral Visual/Parietal-Sensorimotor	Log-linear	−0.1552	0.0033	5.55E-01	−307.32	−317.53
Lateral Visual/Parietal-Auditory/language	Linear	−0.0870	0.0000	5.58E-01	−219.09	−208.24
Lateral Visual/Parietal-Salience	***Log-linear***	**−0.0770**	**−0.0246**	**1.35E-05**	**−326.67**	**−340.54**

Brain Struct Funct. Author manuscript; available in PMC 2016 April 29.

Network	Model	Intercept	Slope	P (Slope)	AIC (Linear)	AIC (Log-linear)
Lateral Visual/Parietal-Frontoparietal R	Log-linear	−0.0046	0.0043	3.81E-01	−411.92	−420.65
Lateral Visual/Parietal-Frontoparietal L	**Log-linear**	**0.0398**	**0.0115**	**2.67E-03**	**−565.58**	**−576.43**
Default-Sensorimotor	***Log-linear***	**−0.0554**	**−0.0381**	**3.10E-16**	**−490.09**	**−515.55**
Default-Auditory/language	Log-linear	0.0008	0.0029	5.67E-01	−394.39	−405.23
Default-Salience	***Log-linear***	**0.0940**	**−0.0231**	**1.62E-08**	**−527.00**	**−546.64**
Default-Frontoparietal R	**Log-linear**	**0.0534**	**0.0220**	**1.78E-08**	**−583.32**	**−605.10**
Default-Frontoparietal L	Log-linear	0.0433	−0.0016	5.75E-01	−775.96	−786.72
Sensorimotor-Auditory/language	***Log-linear***	**0.4428**	**−0.0774**	**2.25E-23**	**−168.11**	**−202.28**
Sensorimotor-Salience	Log-linear	−0.0803	−0.0009	8.89E-01	−219.29	−229.84
Sensorimotor-Frontoparietal R	***Log-linear***	**−0.1397**	**−0.0174**	**1.46E-03**	**−334.79**	**−350.57**
Sensorimotor-Frontoparietal L	Log-linear	−0.0998	0.0061	1.54E-01	−482.86	−494.10
Auditory/language-Salience	Log-linear	−0.0304	0.0106	1.73E-01	−103.25	−114.58
Auditory/language-Frontoparietal R	**Log-linear**	**−0.0609**	**0.0604**	**3.81E-19**	**−230.32**	**−269.37**
Auditory/language-Frontoparietal L	**Log-linear**	**−0.1290**	**0.0316**	**2.15E-11**	**−438.24**	**−462.87**
Salience-Frontoparietal R	Linear	0.0153	0.0000	1.32E-01	−364.87	−353.72
Salience-Frontoparietal L	***Linear***	**−0.0401**	**−0.0001**	**1.56E-03**	**−496.74**	**−484.54**
Frontoparietal R-Frontoparietal L	**Linear**	**0.0962**	**0.0002**	**1.04E-24**	**−628.43**	**−617.10**